Arkadiusz MIASKOWSKI [1], Piotr GAS [2]

University of Life Sciences in Lublin (1), AGH University of Science and Technology (2)
ORCID: 1. 0000-0001-9110-5032; 2. 0000-0003-3969-3281

Modelling of Temperature Distribution in Anatomically Correct Female Breast Cancer

Abstract. The paper aims at the temperature distribution modelling in anatomically correct female breast cancer model using modified Pennes bioheat equation. In our case, a heat transfer in the tumor tissue was considered using different perfusion models i.e. constant, linear and non-linear temperature-dependent blood perfusion model. These temperature-dependent models have been applied in order to account for the strong temperature dependence due to bioregulatory processes inside naturalistic irregular shaped breast tumor. It was found that the temperature patterns distributions do not strongly depend on the perfusion model but they have an impact on temperature rise and its value.

*Streszczenie. Praca ma na celu modelowanie rozkładu temperatury w anatomicznym modelu guza piersi kobiecej przy użyciu zmodyfikowanego równania biocieplnego Pennesa. W naszym przypadku rozważano przenoszenie ciepła w tkance guza przy użyciu różnych modeli perfuzji krwi zależnych od temperatury, a mianowicie: stałego, liniowego i nieliniowego. Modele te zostały zastosowane w celu uwzględnienia silnej zależności od temperatury spowodowanej procesami bioregulacyjnymi wewnątrz naturalistycznego guza piersi o nieregularnym kształcie. Autorzy wykazali, że rozkłady temperatur nie zależą silnie od modelu perfuzji, ale mają wpływ na wzrost temperatury i jej wartość. (**Modelowanie rozkładu temperatury w anatomicznym modelu guza piersi kobiecej**)*

Keywords: hyperthermia, irregular breast cancer, magnetic fluid, Pennes equation, temperature-dependent perfusion, FEM.
Słowa kluczowe: hipertermia, nieregularny guz piersi, ciecz magnetyczna, równanie Pennesa, modele perfuzji, MES.

Introduction

Electromagnetic (EM) field is increasingly used in the treatment of hyperthermia, due to the thermal effect in cancer tissue and proven efficacy in the treatment of tumors of various locations, including female breast tumors. Breast carcinoma is the most frequently diagnosed cancer in women [1,2]. One of the promising oncological therapies, still in the phase of intensive clinical trials, is the so-called magnetic fluid hyperthermia (MFH) [3]. MFH is based on feeding magnetic nanoparticles (MNPs) into cancer and then external EM field of hundreds of kilohertz is applied to induce the tumor temperature in the therapeutic range of $40-45°C$. In this way the MNPs dissipate heat and activate biochemical paths leading to necrosis or apoptosis of malignant cells [4]. The idea of MFH therapy is presented in Fig. 1.

On should realize, that when human tissues are exposed to an alternating EM field, the eddy currents effect is observed due to non-zero conductivity of the tissues [5,6]. That effect describes the process where the energy of an electric current is converted into heat as it flows through the tissues, which finally leads to their heating. In the case of MFH, apart from the eddy currents power losses, at the same time the single-domain nanoparticles magnetic power losses should be considered. The phenomenon of heat dissipation from MNPs is very sophisticated and depends on their concentration, the distribution and the relaxation mechanism in the tumor together with the magnetic field strength and its frequency [7]. However, when comparing both eddy currents and the single-domain nanoparticles magnetic power losses, the effect of the former can be neglected as it is about a hundred times lower [8].

The heat sources in EM-induced hyperthermia can be various types of applicators [9–11], coils [12] and antennas [3–15] operating on radio and microwave frequencies. Depending on the heating technique chosen, the temperature of the tumor may exceed $50°C$. which is associated with the ablation of the cancerous tissue [16–18]. The efficacy of thermal therapy may be enhanced by associated targeted therapy, including radio-, chemo-, immune- or gene therapy [19,20], where nanocarriers might be magnetic particles of different physico-chemical structure [21–24].

During *in-silico* studies on hyperthermia and ablation treatments, cancerous tumors are most often modelled with spheres [2,25–27] or ellipsoids (prolate or oblate spheroids) [28]. However, a recent interest of naturalistic tumor shapes [29] asks about the possibility of taking into account irregular tumor models in thermal therapies procedures.

It should be emphasized that the presented paper ignores important aspects of alternating EM field generation, as they are irrelevant from the point of view of the analysis of various tumor perfusion models. The authors assumed a specific value of power dissipation of MNPs, which results from previous performed *in-silico* and *in-vitro* studies of magnetite nanoparticles immersed in an aqueous solution [30,31].

In the previous work [30], the authors have shown that the different perfusion tumor models effect significantly temperature rise taking into account the spherical tumor model. In the case of irregular shaped tumor such a situation is not straightforward as it is shown in the current work.
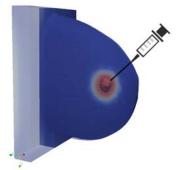

Fig. 1. Idea of magnetic fluid hyperthermia (MFH) treatment: magnetic nanoparticles (MNPs) are fed into tumor and then external EM field is applied

Modified Pennes Equation

A mathematical model dedicated to the numerical analysis of heat transfer in human tissues was proposed by Pennes in the middle of last century [32]. In this model, blood perfusion is assumed to be uniform throughout the tissue and all the heat leaving the artery is absorbed by the local tissue with no venous rewarming. However, the Pennes model is limited to the constant-rate blood perfusion i.e. the arterial temperature is assumed to be equal to the body core temperature. That means Pennes original model

describes blood perfusion with acceptable accuracy if there are no large vessels nearby, like for example, liver [32].

Nevertheless, the vascularized tissue often experiences increased perfusion as temperature increases and it is necessary to consider a more general form of Pennes equation in which the blood perfusion is a function of temperature. The temperature dependent blood perfusion is especially desired when dealing with magnetic fluid hyperthermia and in the cases were high temperature gradients can occurred [8]. In spite of the fact that the temperature-dependent blood perfusion values are still open for discussion, the non-linear ones seem to be the most accurate and provide a faithful representation of the heat dissipation in human tissues [2,3,33,34].

In this work, the temperature distribution was calculated using the modified Pennes equation as [32]:

$$(1) \quad \rho c \frac{\partial T}{\partial t} = \nabla \cdot (k \nabla T) - \rho_{b} c_{b} \rho \omega(T)(T - T_{b}) + \rho Q_{m} + \rho Q_{nano}$$

where ρ is the tissue density, c is the tissue specific heat capacity, k is the tissue thermal conductivity, c_{b} is the blood specific heat capacity, T_{b} is the arterial blood temperature, T is the local temperature, Q_{m} is the heat generation rate (HGR in W/kg) due to the metabolic heat, Q_{nano} is the external power losses due to the eddy current effect and other sources, and $\omega(T)$ is the blood perfusion. In practice, the temperature-dependent perfusion is often defined as so called heat transfer rate and defined as $HTR(T) = \rho_{b} c_{b} \rho \omega(T)$. In our case, the following perfusion models were considered [30]:

a) non-linear model:

$$(2) \quad HTR(T) = 0.4 + 0.4 \exp\left(-\frac{(T-37)^4}{880}\right)\left[\frac{mL}{\min \text{ kg K}}\right]$$

b) linear model:

$$(3) \quad HTR(T) = -1.08 + 0.4T$$
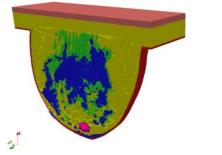
c) constant model:

$$(4) \quad HTR(T) = 0.6$$

Beside the models, see Eqs. (2)–(4), a completely free of no-blood-perfusion model $HTR(T) = 0$, was investigated for comparative analysis.

In the case when dealing with MFH it was shown that the power losses generated by magnetic nanoparticles present in the tumor play a crucial role when comparing to the eddy currents [8]. That is why the external power losses can be expressed as [35]:

$$(5) \quad Q_{nano} = \pi \mu_{0} \chi'' H_{0}^{2} f \rho_{MNP}^{-1} \left[W/kg\right]$$

where χ'' is the average out-of-phase component of susceptibility from each magnetic nanoparticle and f is the frequency of applied electromagnetic field with magnetic field strength equal to H_{0} and ρ_{MNP} is the density of magnetic nanoparticle core.

To specify the thermal conditions at the boundaries of the computational domain the mixed boundary conditions were set in order to describe convection effect as follows [36]:

$$(6) \quad k \frac{\partial T}{\partial n} + h(T - T_{ext}) = F_{boundary}$$

where $\partial T/\partial n$ means the directional derivative of temperature in normal direction, k is the thermal conductivity of skin, h is the heat transfer coefficient and T_{ext} is the external temperature. This boundary condition is appropriate for modeling effects like convection, e.g., the cooling effect of blood in major blood vessels or cooling effect of air around a body. Additionally, model includes exchange of radiative heat with the boundary term of the form [36]:

$$(7) \quad F_{radiation} = \sigma_{SB}(T^4 - T_{ext}^4)$$

where $\sigma_{SB} = 5.67 \cdot 10{-}8$ W/m^2/K^4 is the Stefan-Boltzmann constant.

Above equation can be also expressed as:

$$(8) \quad F_{radiation} = \sigma_{SB}(T - T_{ext})(T + T_{ext})(T^2 + T_{ext}^2)$$

or for small temperature differences, it can be approximated by:

$$(9) \quad F_{radiation} = 4\sigma_{SB}(T - T_{ext})T_{ext}^3$$

Finally, taking the above into account, the mixed boundary condition (6) used in the simulation with coefficient $h = 4\sigma_{SB}T_{ext}^3$ can be written as:

$$(10) \quad k \frac{\partial T}{\partial n} + 4\sigma_{SB}(T - T_{ext})T_{ext}^3 = F_{boundary}$$

Anatomically Correct Female Breast Phantom

In order to get as close as possible to the real disease case, the authors performed calculations using the anatomically correct model of the female breast with irregular shaped cancer. As for the female breast phantom used in this work, it was taken from UWCEM Numerical Breast Phantom Repository (see Fig. 2a) and the following tissues were extracted and coloured: skin – red, muscle – orange, breast fat – yellow, fat – green, breast gland – blue. The breast screening of tumor was provided by Dalian University of Technology, China. In Fig. 2b, it can be seen the tumor model with regard to sphere of radius $r = 10$ mm in order to better visualize tumor's irregular shape. Similar breast phantoms one can find in [3,15,27,29,37] however, the proposed models were simplified to the semi-ellipsoidal block, the semi-sphere or to the anatomically correct shape without naturalistic breast tissues.
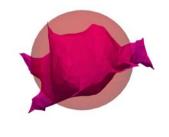
a)   b)

Fig. 2. a) Female breast phantom xy-cross section including irregular shaped tumor, and b) the tumor model with regard to sphere of radius $r = 10$ mm
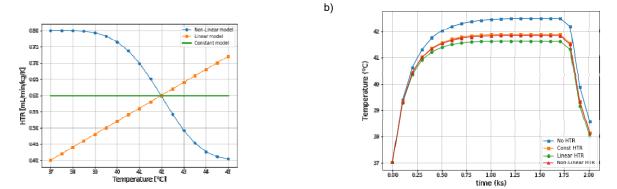
a)

b)

Fig. 3. a): The different perfusion models as presented in Eqs. (2)–(4) [30], and b) temperature over time in the tumor centre for different blood perfusion models

In this paper the anatomically correct female breast model was used together with naturalistic tumour model. Analysed tumor blood perfusions rates are depicted in Fig. 3a. Tissue parameters were taken from freely available databases [38] and their physical para-meters are gathered in Table 1 for frequency $f = 100$ kHz. Importantly, the HTR coefficient for tumor, given in Table 1, is variable due to used blood perfusion model as described in Eqs. (2)–(4).

Table 1. Physical parameters of the breast phantom [38]

Quantity	Blood	Breast fat	Breast gland
ρ_b, ρ [kg/m³]	1050	911	1041
c_b, c [J/kg/K]	3617	2348	2960
k [W/m/K]	0.5169	0.209	0.334
HTR [mL/min/kg]	10 000	47	150
HGR [W/kg]	0	0.728	2.323

Quantity	Fat	Muscle	Skin	Tumor
ρ[kg/m³]	911	1090	1109	1090
c [J/kg/K]	2348	3421	3391	3421
k [W/m/K]	0.211	0.495	0.372	0.495
HTR [mL/min/kg]	32.71	36.74	106	var
HGR [W/kg]	0.506	0.906	1.648	100

Simulation Results

In order to numerically investigate the described problem a commercially available Sim4Life software [36] was employed. In our case, the Thermal Solver integrated into Sim4Life platform was used to simulate the thermal effects in the particular setup as presented above. From mathematical point of view, the thermal solver is based on the extended form of diffusion differential equation with specific boundary conditions.

In our case the initial conditions, T_0, understood as temperature for each individual breast tissue at the start of the simulation was set to $37°C$, the overall (background) temperature was set to $25°C$ and the heat transfer coeffi-cient h was set to $h = 5$ W/m²/K. In addition, it was assumed that the power density generated by MNPs (placed inside the tumor) is homogenous and it is at the level of $Q_{nano} = 100$ W/kg. This value is already recognized as a minimum one, which is desired to reach the therapeutic temperature $42°C$ [30]. In this way, it was assumed that magnetic nano-particles are uniformly distributed in the tumor volume as found in many similar papers [31]. However, heterogeneous nanofluid spatial distribution inside tumor tissue is also the subject of intensive hyperthermia studies [39]. One should also realise that the coefficients of the blood perfusion models have been chosen so that their common point falls to $42°C$ i.e. at therapeutic temperature, which seems to be relevant assumption.

Fig. 3b indicates that the therapeutic temperature profiles in the middle of the tumor was reached in all cases except the one where there is no perfusion – in this case the temperature was the highest, as expected, and it was about $43°C$. Moreover, for the constant and linear perfusion models the temperature over time is almost the same. From computational point of view such a situation is very important as every nonlinear model is very time-consuming. Therefore, it is advisable to use simplification models with linear or constant tumor blood perfusion rates.

In Fig. 4 can be seen the example cross-section temperature distribution in the breast model in the steady-state after 1800 seconds due to heat source from magnetic nanoparticles Q_{nano}. One can notice that temperature about $42°C$ inside the tumor and its vicinity has been reached for every perfusion model under consideration. It is clear that heterogeneous temperature distribution in the tumor vicinity can be observed because of irregular tumor shape as well as due to different properties of the tissues surrounding the tumor. To better visualise these heterogeneous patters the circle of radius $r = 10$ mm has been added to the drawings.
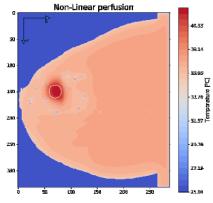

Fig. 4. The xy-cross section of temperature distribution passing through the middle of the tumor in the steady-state for non-linear perfusion model

Summary

In present paper, the temperature distribution modelling in anatomically correct female breast cancer with different blood perfusion rates has been presented. It was found that the temperature patterns distributions do not strongly depend on the perfusion model (i.e. constant-, linear- non-linear and perfusion-free model) but the application of the particular model has an impact on temperature rise ratio and its value. It was shown that temperature rise ratio depends on the applied perfusion model. Moreover, it is worth noticing that the application of the non-linear model and the constant one in the modified Pennes bio-heat

equation, gave the same temperature rise in the function of time. This result can be very useful from computational point of view i.e. non-linear models are often time- and memory-consuming models. Therefore, the authors recommend the use of simplified models with linear or constant perfusion rates during the hyperthermia treatment planning.

Authors: *dr hab. inż. Arkadiusz Miaskowski, PhD, University of Life Sciences in Lublin, Department of Applied Mathematics and Computer Sciences, ul. Akademicka 13, 20-950 Lublin, Poland, E-mail: arek.miaskowski@up.lublin.pl, dr hab. inż. Piotr Gas, PhD, AGH University of Science and Technology, Department of Electrical and Power Engineering, al. Mickiewicza 30, 30-059 Krakow, Poland, E-mail: piotr.gas@agh.edu.pl*

REFERENCES
[1] Siegel R.L., et al., Cancer statistics, 2021, *CA: A Cancer Journal for Clinicians*, 71 (2021), No. 1, 7–33.
[2] Gas P., Miaskowski A., Subramanian M., In silico study on tumor-size-dependent thermal profiles inside an anthropomorphic female breast phantom subjected to multi-dipole antenna array, *International Journal of Molecular Sciences*, 21 (2020), No. 22, 8597. DOI:10.3390/ijms21228597,
[3] Sawicki B., Miaskowski A., Nonlinear higher-order transient solver for magnetic fluid hyperthermia, *Journal of Computational and Applied Mathematics*, 270 (2014), 143–151.
[4] Minnaar C.A., Szasz A., Forcing the Antitumor Effects of HSPs Using a Modulated Electric Field, *Cells*, 11 (2022), 1838.
[5] Gas P., Temperature inside tumor as time function in RF hyperthermia, *Przeglad Elektrotechniczny*, 86 (2010), No. 12, 42–45.
[6] Syrek P., et al., Eddy Currents Distribution in Upper Extremities During Magnetotherapy, In: *2019 11th International Symposium on Advanced Topics in Electrical Engineering (ATEE)*, IEEE, (2019), 1–4. DOI: 10.1109/ATEE.2019.8724967
[7] Carrey B., et al., Simple models for dynamic hysteresis loop calculations of magnetic single-domain nanoparticles: Application to magnetic hyperthermia optimization, *Journal of Applied Physics*, 109 (2011), No. 8, 083921.
[8] Miaskowski A. Subramanian M., Numerical Model for Magnetic Fluid Hyperthermia in a Realistic Breast Phantom: Calorimetric Calibration and Treatment Planning, International Journal of Molecular Sciences, 20 (2019), No. 18, 4644.
[9] Geyikoglu M.D., Cavusoglu B., Microwave hyperthermia with X band flexible hyperthermia applicator for bone and joint cancer treatment, *Journal of Electromagnetic Waves and Applications*, 36 (2022), No. 9, 1285–1297.
[10] Kologeropoulos A., Tsitsas N., Excitation of a layered medium by *N* sources: Scattering relations, interaction cross sections and physical bounds, Quarterly of Applied Mathematics, 79 (2021), pp. 335–356.
[11] Portosi V., et al., Feasibility investigation of low-cost microwave needle applicator for thermal ablation cancer therapy, In: *2020 IEEE International Symposium on Medical Measurements and Applications (MeMeA)*, IEEE, (2021), 1–6.
[12] Lopez J.I., et al., Estimation of Electrical Conductivity from Radiofrequency Hyperthermia Therapy for Cancer Treatment by Levenberg Marquardt Method, *Communications in Computer and Information Science*, 1195 (2020), 142–154.
[13] Nizam-Uddin N., et al., Towards an efficient system for hyperthermia treatment of breast tumors, *Biomedical Signal Processing and Control*, 71 (2022), 103084.
[14] Suseela S., Wahid P., Breast cancer hyperthermia using a grid array applicator, In: *2020 SoutheastCon*, (2020), 1–4.
[15] Ling W.V., et al., SAR distribution of non-invasive hyperthermia with microstrip applicators on different breast cancer stages, *Indonesian Journal of Electrical Engineering and Computer Science*, 22 (2021), 232–240.
[16] Ashour A.S., et al., Optimal power for microwave slotted probes in ablating different hepatocellular carcinoma sizes, *Computers in Biology and Medicine*, 127 (2020), 104101.
[17] Radmilovic-Radjenovic M., el al., Finite element analysis of the effect of microwave ablation on the liver, lung, kidney, and bone malignant tissues, *EPL*, 136 (2021), 28001.
[18] Trujillo-Romero C.J., et al., Double Slot Antenna for Microwave Thermal Ablation to Treat Bone Tumors: Modeling and Experimental Evaluation, *Electronics*, 10 (2021), 761.
[19] Aziz O.A.A., et al., Superparamagnetic iron oxide nanoparticles (SPIONs): preparation and recent applications, *Journal of Nanotechnology Advanced Material*, 8 (2020), No. 1, 21–29.
[20] Orrico A., et al., Controlled photothermal therapy based on temperature monitoring: theoretical and experimental analysis, In: *2021 IEEE International Symposium on Medical Measurements and Applications (MeMeA)*, IEEE, (2021), 1–6.
[21] Oehlsen O. et al., Approaches on Ferrofluid Synthesis and Applications: Current Status and Future Perspectives, *ACS Omega*, 7 (2022), No. 4, 3134–3150.
[22] Theodosiou M., et al., Iron oxide nanoflowers encapsulated in thermosensitive fluorescent liposomes for hyperthermia treatment of lung adenocarcinoma, *Scientific Reports*, 12 (2022), No. 1, 1–15.
[23] Szczech M., Experimental studies of magnetic fluid seals and their influence on rolling bearings, *Journal of Magnetics*, 25 (2020), No. 1, 48–55.
[24] Yu X., et al., Effect of chromium ion substitution of ZnCo ferrites on magnetic induction heating, Journal of Alloys and Compounds, 830 (2020), 154724.
[25] Paruch M., Sensitivity analysis and the inverse problem in the mathematical modelling of tumor ablation using the interstitial hyperthermia. AIP Conference Proceedings, 2239 (2020), No. 1, 020038. DOI: 10.1063/5.0007828
[26] Michalowska-Samonek J., et al., Numerical analysis of high frequency electromagnetic field distribution and specific absorption rate in realistic breast models, *Przeglad Elektrotechniczny*, 88 (2012), No. 12b, 97–99.
[27] Neto C.D., et al., A simplified mathematical model to predict the human breast thermal response, *26th International Congress of Mechanical Engineering (COBEM 2021)*, IEEE, (2021), 1070.
[28] Polychronopoulos N.D., et al., A Computational Study on Magnetic Nanoparticles Hyperthermia of Ellipsoidal Tumors, *Applied Sciences*, 11 (2021), 9526.
[29] Byrd B.K., et al., The shape of breast cancer, *Breast Cancer Research and Treatment*, 183 (2020), 403–410.
[30] Gas P., Miaskowski A., Dobrowolski D., Modelling the tumor temperature distribution in anatomically correct female breast phantom, *Przeglad Elektrotechniczny*, 96 (2020), No. 2, 146–149. DOI: 10.15199/48.2020.02.35
[31] Raouf I., Gas P., Kim H.S., Numerical Investigation of Ferrofluid Preparation during In-Vitro Culture of Cancer Therapy for Magnetic Nanoparticle Hyperthermia, *Sensors*, 21 (2021), 5545. DOI: 10.3390/s21165545
[32] Pennes H.H., Analysis of tissue and arterial blood temperature in the resting human forearm, *Journal of Applied Physiology*, 1 (1948), No. 2, 93–122.
[33] Kengne E., et al., A mathematical model to solve bio-heat transfer problems through a bio-heat transfer equation with quadratic temperature-dependent blood perfusion under a constant spatial heating on skin surface, *Journal of Biomedical Science and Engineering*, 7 (2014), No. 9, pp. 721–730.
[34] Lang B., et al., Impact of nonlinear heat transfer on temperature control in regional hyperthermia, *IEEE Transactions on Biomedical Engineering*, 46 (1999), No. 9, 1129–1138.
[35] Rosensweig R.E., Heating magnetic fluid with alternating magnetic field, *Journal of Magnetism and Magnetic Materials*, 252 (2002), 370–374.
[36] Sim4Life, Sim4Life Manual, Realise 6.2., (2021)
[37] Neira L.M., et al., Human breast phantoms: Test beds for the development of microwave diagnostic and therapeutic technologies, *IEEE Pulse*, 8 (2017), No. 4, 66–70.
[38] Hasgall P.A., et al., IT'IS Database for thermal and electromagnetic parameters of biological tissues, Version 4.1, Feb 22, 2022.
[39] Tang Y.D., Effect of injection strategy for nanofluid transport on thermal damage behavior inside biological tissue during magnetic hyperthermia, International Communications in Heat and Mass Transfer, 133 (2022), 105979.